

ESTABLISHMENT OF A MODEL SYSTEM TO TEST THE IMPACT OF  
DNA SENSING BY AIM2 ON EPITHELIAL CELL DIFFERENTIATION

By

SYDNEY AUBRIANNA NOELLE VERDUGO

---

A Thesis Submitted to The W.A. Franke Honors College

In Partial Fulfillment of the Bachelor's degree  
With Honors in

Molecular and Cellular Biology

THE UNIVERSITY OF ARIZONA

M A Y 2 0 2 3

Approved by:

---

Dr. Justin E. Wilson  
Department of Immunobiology

## Abstract

The global incidence of Inflammatory Bowel Diseases (IBD) has been on the rise. In our lab, we investigate how intestinal inflammatory responses are regulated by the innate pattern recognition receptor, Absent in Melanoma 2 (AIM2), which acts as a cytosolic dsDNA sensor. AIM2 has previously been implicated in both IBD as well as colorectal cancer. However, while AIM2 has mainly been characterized in immune cells, AIM2 is also present in epithelial cells. Preliminary evidence from our lab has shown that *Aim2*<sup>-/-</sup> 3D small intestine epithelial cell organoid cultures display a marked decrease in epithelial tuft cells as evidenced by loss of an associated tuft cell marker, *Dclk1*. Given these results, it was important to determine the mechanism by which AIM2 may regulate the differentiation of epithelial cells. To test the hypothesis that AIM2 impacts epithelial cell differentiation through its dsDNA sensing function, we optimized a 2D small intestine organoid system, which allows for cytosolic delivery of small molecules via transfection. Utilizing this 2D system, we first confirmed that the tuft cell-inducing cytokine IL-4 induces an upregulation of the tuft cell master transcription factor, *Pou2f3*. In response to dsDNA, there was a marked increase in *Il13ra1*, which encodes for the receptor shared by IL-4 and the related cytokine IL-13. These results suggest that AIM2 may promote expression of the receptor that is essential to tuft cell differentiation. These studies reveal a new mechanism by which immune sensing may play a pivotal role in intestinal epithelial homeostasis.

## Introduction

Over the span of the last 30 years, the global incidence of Inflammatory Bowel Disease (IBD), consisting primarily of ulcerative colitis and Crohn's disease, has increased by 85% <sup>(1)</sup>. Characteristics of these diseases include abdominal pain, diarrhea, fatigue, and passage of blood during bowel movements <sup>(2)</sup>. There are many factors both environmental and genetic that may play a role in the onset of IBD. For example, a mutation in NOD2, another pattern recognition receptor, has been previously characterized as a contributing factor in Crohn's disease <sup>(3)</sup>. NOD2 also acts as a microbial sensor, by recognizing a component of peptidoglycan found within bacterial cell walls (muramyl dipeptide). NOD2 is a part of the Nod-Like Receptor Family (NLR), many of which contain pyrin domains and some having the capability to form inflammasomes. This is what initially led to further interest in other pattern recognition receptors. Another component of these diseases is dysregulation between type 1 and type 2 inflammation, which are critical for balancing promotion and resolution of different types of inflammation. This balance can be altered based on the intestinal environment and the microorganisms that inhabit it. Changes in the normal intestinal microbiome can give rise or be a result of inflammation, along with an intolerance to commensal organisms. Another contributor could be a loss of integrity within the barrier of the intestinal epithelium leading to bacteria infiltration. Based off of this information, it is pertinent that we better understand the molecular links between microbial sensing and inflammation progression in order to better understand the onset and progression of IBD.

The main protein of interest in our lab is Absent in Melanoma 2 (AIM2). AIM2 is a microbial sensing pattern recognition receptor that facilitates innate immune activation through two known functions. The most-well documented function of AIM2 is as a DNA sensor. When double stranded DNA (dsDNA) enters the cytosol, AIM2 recognizes and binds to it. From there, AIM2 recruits ASC and Caspase-1 to create the multi-protein complex termed the inflammasome. The AIM2 inflammasome then cleaves pro-caspase IL-18 and IL-1 $\beta$  into their active forms to initiate inflammation, pathogen clearance, and epithelial repair <sup>(4,5)</sup>. AIM2 also functions as an inhibitor of DNA-dependent Protein Kinase (DNA-PK), which in turn leads to restriction of AKT phosphorylation and activation. Since AKT is a known oncogene, AIM2 functions in this manner by preventing cellular proliferation and inhibiting pro-survival pathways to restrict tumorigenesis <sup>(6)</sup>. Both functions of AIM2 have been previously found within immune cells and epithelial cells.

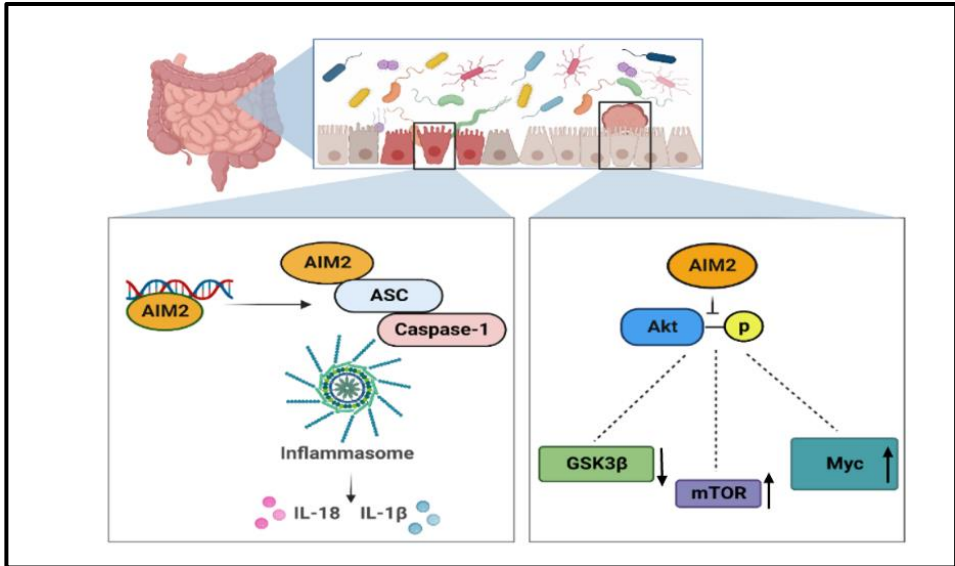


**Figure 1: Functions of AIM2.** AIM2 primarily functions as a dsDNA sensor. AIM2 binds dsDNA in the cytosol and recruits ASC and Caspase-1 to form the inflammasome. The inflammasome then initiates cleavage of IL-18 and IL-1β to initiate inflammatory responses. AIM2 also acts as a tumor suppressor by inhibiting the phosphorylation of AKT, thus restricting tumorigenesis and cell-survival pathways. Figure created with BioRender

Both the small intestine and the colon are comprised of crypt-like structures that make up the intestinal epithelium. At the bottom of these crypts lies the stem cell niche, where these stem cells can differentiate in three different ways. Either they can: 1) terminally differentiate into two separate transit-amplifying cells; 2) one can remain in a stem cell state, while the other becomes a transit-amplifying cell, or 3) both divide into two stem cells (7). As the cells move up the sides of the crypt, they transition from stem cells into transit-amplifying cells. As these cells continue up the crypt, they will eventually terminally differentiate into distinct epithelial cellular sub-types that provide physical barriers and display specialized functions that help the intestines maintain homeostasis. An important trait of the intestinal epithelium and these cellular sub-types is that they can respond to environmental signals such as microbes (both pathogenic and commensal) and localized immune activation. These crypts contain cell types such as goblet cells, Paneth cells, enterocytes, stem cells, enteroendocrine cells and tuft cells (8). Each cell type is responsible for different roles within the intestinal epithelium. For example, goblet cells are particularly pertinent for producing mucus, and tuft cells have microbial sensing capability. A common trait of IBD is dysregulation between the microbiome, immune system, and these various epithelial cells.

In our lab we are focused on one of these epithelial sub-types, tuft cells. Tuft cells are a rare population that exist throughout the body such as the lungs, thymus, and the trachea. Tuft cells are also found within both the small intestine and the colon, although they may serve different functions in these tissue sites. For example, tuft cells are important for promoting a type 2 inflammatory response particularly in the small intestine, which is pertinent to host defense against helminth and protozoan infections. Tuft cells are part of a feed-forward loop involving type II innate lymphoid cells (ILC2s), which dramatically promote further stem cell differentiation into tuft cells (tuft cell hyperplasia). Tuft cells express a surface receptor for succinate, which is normally found intracellularly and is pertinent for the Krebs cycle. However, extracellular succinate produced by microbes can be sensed by the succinate receptor (SUCNR1) on tuft cells, thus causing tuft cells to secrete the alarmin IL-25. It should be noted as

well that some helminths can activate this response independent of succinate. This indicates that other cell triggers exist but have yet to be identified. IL-25 then activates and recruits ILC2's, which secrete type 2 inflammatory cytokines IL-4 and IL-13. Once IL-4 and IL-13 are secreted, they then stimulate their associated receptors on intestinal stem cells residing at the bottom of the crypt, leading to preferential tuft cell hyperplasia<sup>(9,10)</sup>. This response also induces activation and hyperplasia of goblet cells and initiates remodeling of the intestinal epithelium to both promote removal of the helminth infection and sustain the type 2 inflammatory response if necessary. One important piece to note is that the IL-13 and IL-4 receptors share receptor components, and both of these cytokines can induce tuft cell differentiation<sup>(11)</sup>. The tuft cell lineage can be tracked using *DCAMKL1* (*Dclk1*) along with the tuft cell master transcription factor, *Pou2f3*. Tuft cells have recently been implicated in helping to mitigate experimental IBD through their promotion of type 2 inflammatory response, thus counteracting the overproduction of both type 1 and type 3 inflammatory responses seen in these diseases<sup>(10)</sup>. This and other recent reports highlight that tuft cells have an important function beyond combating parasitic infection.

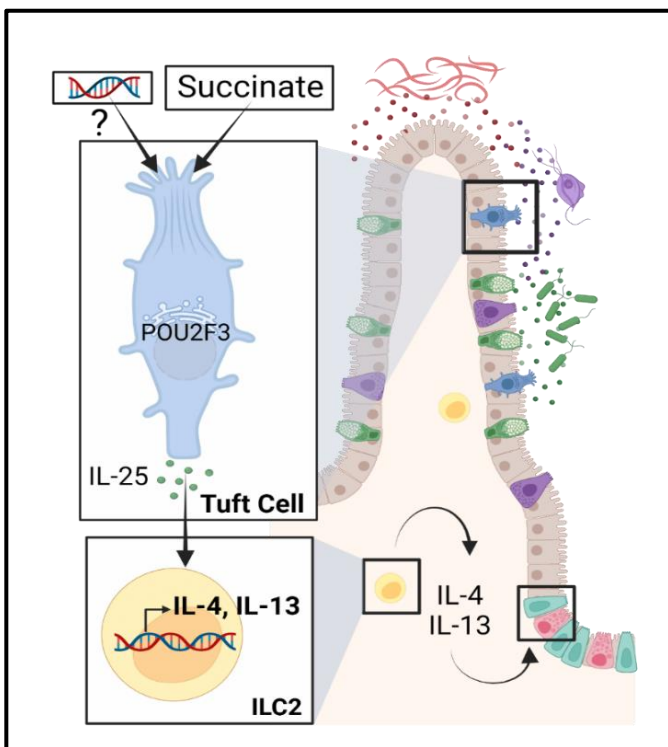


**Figure 2: Model of the Tuft Cell-ILC2 Circuit.** Extracellular succinate is recognized by the tuft cell surface succinate receptor (SUCNR1). After succinate is sensed, the tuft cell releases the alarmin IL-25. Innate type 2 lymphoid cells (ILC2s) are then activated and recruited in response to IL-25 secretion. ILC2s then secrete type 2 inflammatory cytokines IL-4 and IL-13. IL-4 and IL-13 then go on to stimulate their associated receptor complex, IL4ra and IL13ra1, on the stem cell niche to promote further differentiation of tuft cells. Helminth infections can elicit the type 2 inflammatory response independent of succinate. Based on our previous findings, AIM2 is implicated in tuft cell promotion and thus, we propose that AIM2's dsDNA sensing function may play a role in tuft cell development. Figure created with BioRender.

Preliminary evidence from our lab identified a marked decrease in *Dclk1*-expressing tuft cells in *Aim2*<sup>-/-</sup> 3D small intestine organoids and in succinate-fed *Aim2*<sup>-/-</sup> mice. This suggests that AIM2 plays a role in promoting intestinal tuft cell differentiation, however, the mechanism by which this occurs is still unknown. Given these findings, it would be imperative to learn if AIM2's DNA sensing ability is responsible for driving epithelial cell differentiation, which may lead to a possible avenue to help mitigate IBD. This work would also provide new insights into how microbial sensing and/or damage

signals may play a role in determining the fate of epithelial cells to impact immune regulation.

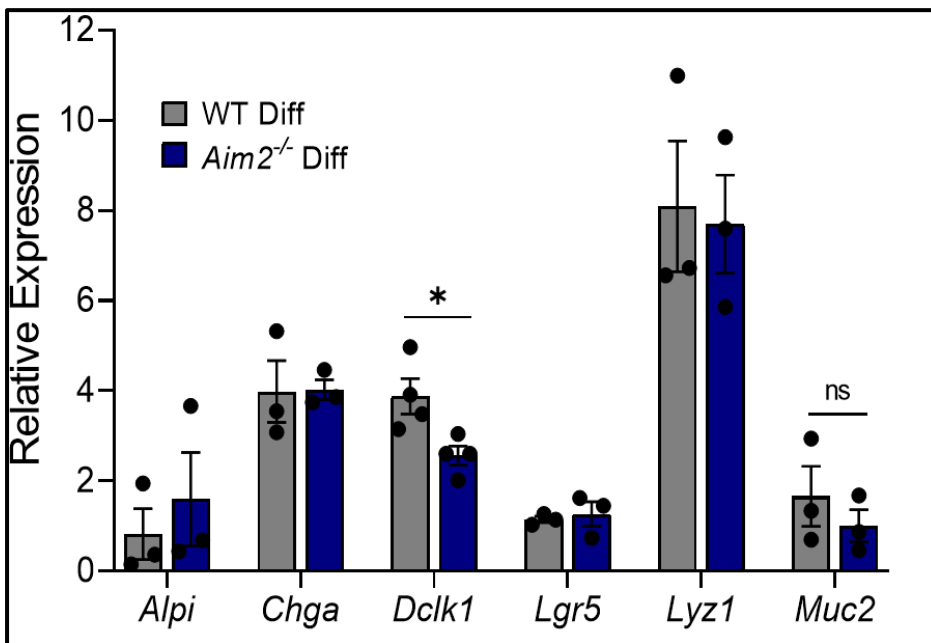


**Figure 3: *Aim2*<sup>-/-</sup> 3D small intestine epithelial cell organoid cultures show decrease in *Dclk1*.** 3D small intestine organoids were made from small intestines from WT and *Aim2*<sup>-/-</sup> mice. Small intestine crypts were dissociated and then embedded in Matrigel. 3D small intestine organoids were differentiated from stem cell-enriched spheroids by removing Wnt-3a. The differentiated organoids were cultured to

Day 5 prior to collection for RNA isolation. \* $p < 0.05$  and the above graph represents  $n=3$  independent experiments. Errors bars represent standard error of the mean (SEM). GraphPad Prism V.9.4.1 was used to generate figure and perform statistical analysis. (Data generated by Stephanie L. Tribble)

## Methods

**2D Organoid Cell Cultures:** 96-well plate was coated with Matrigel/AdvDMEM/F12 at a 1:40 ratio. 50  $\mu$ l was added per well into a 96-well plate and placed into an incubator (37°C) until seeding. Small intestines from C57BL/6 mice were extracted and flushed with 1X PBS and maintained in 1X PBS with Penicillin/Streptomycin until further processing. Small intestines were then fileted open and gently scraped using a glass slide. From there, they were placed into a 2<sup>nd</sup> buffer (1X PBS, 1M DTT, 0.5M EDTA, 10mM Y-27632, 500X Primocin) and placed horizontally on ice for 30 minutes, gently rocking every 10 minutes. After 30 minutes, the tubes containing the small intestines were shaken continuously for 2 minutes. The intestines were removed and placed into another buffer (1X PBS, 0.5M EDTA) horizontally on ice for 15 minutes. After 15 minutes, the tubes were shaken continuously for 2 minutes. This final step was repeated two more times with two sequential and separate tubes containing the same buffer as above. From there, the two buffers containing the most crypts and least villi were chosen. The contents of these two buffers were combined and centrifuged at 4°C for 7 minutes at 300g. Next, the liquid was aspirated, leaving behind a cell pellet. The pellet was resuspended in 10mL of full growth media (DMEM, 10% FBS, 1% P/S) and centrifuged again at 4°C for 7 minutes at 300g. This process was repeated two more

times. The pellet was then resuspended in full growth media one last time and filtered through a 100 µm cell strainer. Next, the media containing cells were filtered two more times using 70 µm cell strainers. Cells were centrifuged again at 4°C for 7 minutes at 300g. The full growth media was aspirated leaving behind the cell pellet. The pellet was then resuspended in seeding media (rmEGF, LDN-193189, 500X Primocin, HEPES, Glutamax, B27, N-acetylcysteine, R-spondin 1 Conditioned Media, AdMEM-F12, CHIR 99021, Y-27632). The non-adherent Matrigel/ AdvDMEM/F-12 was dispensed out of the pre-coated 96 well plate, and 50 µl of cells were plated per well. The media was changed daily (rmEGF, LDN-193189, 500X Primocin, HEPES, Glutamax, B27, N-acetylcysteine, R-spondin 1 Conditioned Media, AdMEM-F12). The 2D organoids were stimulated on Day 2 post-plating and were harvested or fixed on Day 4 or Day 5 as indicated.

**Mouse Background:** Wild-type (WT) C57BL/6 mice were originally obtained from the Jackson Laboratories (Bar Harbor, ME) and maintained at UNC Chapel Hill for more than 9 generations prior to being reestablished at the University of Arizona. The *Aim2* knockout (*Aim2*<sup>-/-</sup>) mice were generated by Ingenious Targeting Laboratory (Ronkonkoma, NY) on the C57BL/6 background via targeted replacement of the *Aim2* coding region with a neomycin resistance gene through homologous recombination. Sequences used for PCR-based *Aim2*<sup>-/-</sup> mouse genotyping are as follows: neomycin (KO) forward, GGAACCTTCGCTAGACTAGTACGCGTG; neomycin (KO) reverse, CAACATTGTACAGATTGAGCAGG; *Aim2* (WT) forward, GATGGAGAGTGAGTACCGGGAAATGCTGTT; and *Aim2* (WT) reverse, TCTGCAAGTAGATTGGAGACAGACTCTGGTGA, resulting in a 450-bp band for the wild type and a 250-bp band for the targeted *Aim2* knockout when PCR analysis is performed on the genomic DNA.<sup>(2)</sup>

**DNA Transfection:** 1mL of Opti-mem, Lipofectamine 2000, and 2D Organoid Culture Media (rmEGF, LDN-193189, 500X Primocin, HEPES, Glutamax, B27, N-acetylcysteine, R-spondin 1 Conditioned Media, AdMEM-F12) was brought to room temperature. Two 0.5mL tubes were labeled with either DNA (diluted poly(dA:dT) with lipofectamine 2000) or LIPO (diluted lipofectamine 2000 with Opti-mem). The poly(dA:dT) was prepared by taking an aliquot of poly dA:dT stock at 1 mg/mL and diluting to the desired amount of poly(dA:dT) stock into Opti-mem to get the final concentration (1 µg/ml). The lipofectamine 2000 was prepared by taking the lipofectamine 2000 and diluting into Opti-mem (utilize 2.5 µl Lipofectamine 2000/ 1 µg of poly(dA:dT) and Lipofectamine 2000 is diluted 1:20 in Opti-mem). Both tubes were gently mixed with the tip of a P20, slowly pipetting up and down. The tubes were then incubated at room temperature for 5 minutes. Next, to encapsulate the poly(dA:dT) in the lipofectamine 2000, an equal volume of the lipofectamine 2000 prep was added into the poly(dA:dT) prep. The tubes were then gently mixed using the tip of a P200 pipette, slowly pipetting up and down. Next, an equal volume of Opti-mem was added into the Lipofectamine 2000 prep. Again, the tube was gently mixed using the tip of a P200 pipette, slowly pipetting up and down. Both tubes were allowed to sit for 10 minutes at

room temperature. The media from the 2D organoid tissue culture plate was removed and replaced with 45  $\mu$ l of 2D media per well. 5  $\mu$ l of the diluted lipofectamine with or without poly(dA:dT) was added into the appropriate wells (5  $\mu$ l of diluted poly(dA:dT) was added to the wells to stim with DNA, 5  $\mu$ l of diluted lipofectamine 2000 was added into the wells to stim with Lipofectamine as a vehicle control, 5  $\mu$ l of Opti-mem was added into the untreated wells to act as a negative control). The 2D organoids were then left overnight. Media was changed the next day and 50  $\mu$ l of 2D organoid culture media was used for each subsequent change until the end of the experiment.

**IL-4 Stimulation:** 2D organoid culture media (see above) was brought to room temperature. The rmlL-4 stock (100 mg/mL) was thawed to room temperature. A 15mL canonical tube was labeled with IL-4 2D organoid culture media, and the number of tubes that needed for a 48-hour stimulation was prepared in advance. The appropriate amount of 2D organoid culture media (see above) was aliquoted into each labeled tube. The final concentration of rmlL-4 that was diluted in 2D organoid culture media was 50 ng/ml. The rmlL-4 was added to the 2D organoid culture media aliquoted right before stimulating. The media was removed from the 2D organoid tissue culture plate, and 50  $\mu$ l of rmlL-4 2D organoid culture media was added to the desired wells. The plate was then left overnight. For a 48-hour stimulation, the above process was repeated the next day, with the added rmlL-4 prepared the day of the media change to ensure cytokine bioactivity.

**RNA Isolation:** In order to prep the 2D organoids for RNA collection, the media in the 96-well 2D organoid tissue culture plate was flicked out. 30  $\mu$ l of 1X PBS was added to each well and gently swirled around the plate. The 1X PBS was then removed from the 2D organoid tissue culture plate. Next, 15  $\mu$ l of Thermo RNA PureLink lysis buffer was added to each well of the 2D organoid tissue culture plate and incubated for 5 minutes. Once done, 15  $\mu$ l of 70% ethanol was added into each well containing the 15  $\mu$ l of lysis buffer. In total, there was 30  $\mu$ l of the lysis buffer/ 70% ethanol mixture per well. The 30  $\mu$ l lysis buffer/ 70% ethanol mixture was collected and placed into a labelled tube. The RNA was then extracted according to the Thermo PureLink RNA extraction protocol.

**cDNA:** To convert RNA to cDNA, a spectrometer was first used to measure the amount of RNA isolated from each sample. From there, the amount of molecular-grade water, RNA and Iscript Master Mix was calculated for each reaction according to the Iscript cDNA synthesis kit protocol (Bio-Rad). In total, the final volume in the tube was 20  $\mu$ l. For our purposes, the RNA concentration that we used was 200 ng. The reagents were then mixed together and run on a thermocycler according to the Iscript protocol (1. 25°C for 5 minutes, 2. 46°C for 20 minutes, 3. 95°C for 1 minute, 4. 12°C indefinite hold). Once completed, 180  $\mu$ l of molecular-grade water was added to the sample bringing the final volume of cDNA to 200  $\mu$ l per sample. The samples were then stored at 4°C until running the RT-qPCR reactions.

**RT-qPCR:** To run the RT-qPCR reaction, TaqMan Master Mix and desired TaqMan primers (ThermoScientific) were thawed on ice. The amount of TaqMan Master Mix and



primers needed for the reaction was calculated with all samples run in technical duplicates. Each well of a 96-well RT-qPCR plate contained 5  $\mu$ l of TaqMan Master Mix and 0.25  $\mu$ l of the desired TaqMan primer pair. Next, 4.75  $\mu$ l of the appropriate cDNA was added to each well. In total, the final volume in the well was 10  $\mu$ l. GAPDH was used as an internal reference gene. The TaqMan Master Mix and Primer combination was then centrifuged to combine all of the reaction components and cDNA in each well. The plate was then placed into RT-qPCR machine and relative gene expression was determined through the ddCt method.

## Results

Preliminary evidence from our lab showed that the absence of AIM2 results in a significant reduction in the amount of tuft cells that are produced in organoid cultures and in succinate-fed mice. Given this information and knowing that AIM2's primary function is to sense double-stranded DNA, the next step was to determine if this function of AIM2 is responsible for the promotion of tuft cells. In order to start answering the question of how this occurs from a mechanistic standpoint, we needed to adopt a new in vitro system that would allow for transfection of DNA molecules into the cytosol where AIM2 resides. All of our in vitro preliminary data was obtained using a 3D organoid system, where the main limitation is that the cells are encased in a dome of Matrigel that obstructs liposome-mediated transfections. Given that AIM2 is intracellular, the 3D organoid system is harder to transfect cells uniformly and ensure that the transfected molecules would make it inside the cells in the first place. We adopted a 2D organoid system developed by our collaborator Curtis Thorne, Ph.D. (CMM/UA) and optimized this system to begin to address the DNA sensing function of AIM2 during this process. The main advantage of a 2D organoid system is that the cells create a flat monolayer, thus allowing for direct access to the apical side of the cell to perform uniform transfections that would be ensured to enter the inside of the cell. Another main advantage of the 2D organoid system is that the 96 well format allows for high-throughput treatment conditions and microscopy-based analysis.

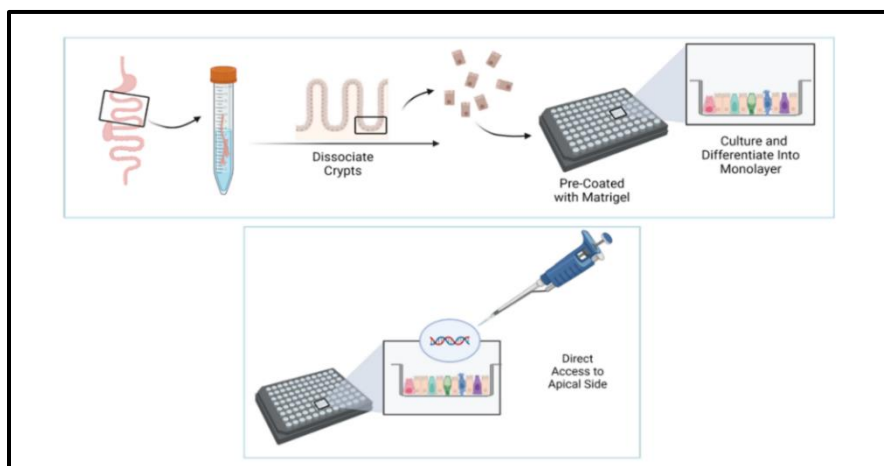


**Figure 4: Schematic of the 2D organoid system approach.**

Small intestines are first isolated from WT mice. Following the 2D small intestine organoid protocol, the crypts were dissociated and then seeded onto a 96-well plate coated with a thin layer of Matrigel. The cells were allowed to differentiate and form the monolayer for 72 hours prior to stimulation. The cells were then

harvested for total RNA 48 hours after stimulation. Figure created with BioRender.

## Pou2f3 is upregulated in response to IL-4

*Pou2f3* is the master transcription factor for intestinal tuft cell development. Both IL-4 and IL-13 are the predominant inducers of *Pou2f3* expression and tuft cell differentiation, which has been demonstrated in both 3D organoids and in mouse models. Based on this knowledge, we next tested if IL-4 could promote tuft cell expansion in our 2D organoid system, similar to what has been described in 3D organoids. This was an important first step in determining if the 2D small intestine organoid system has the same biological relevance as the 3D system. Another key element for this approach involved optimizing RNA isolation from the 2D organoids, where IL-4-induced expression of *Pou2f3* served as a benchmark to ensure that our technique was sound. An increase in IL-4-induced *Pou2f3*, would theoretically indicate an increase in tuft cells is present. To test this, 2D small intestine organoids were differentiated for 72 hours followed by treatment with IL-4 for 48 hours. Total RNA was then isolated, and *Pou2f3* expression was measured by RT-qPCR. After stimulating with IL-4, there was a significant increase in *Pou2f3* expression compared to untreated organoids, thus demonstrating that small intestine organoids grown in 2D can differentiate into tuft cells in response to IL-4.

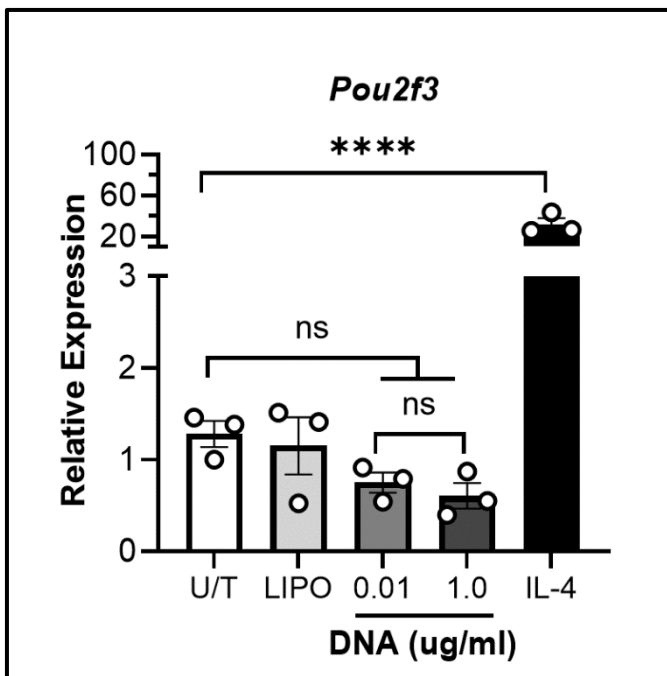


**Figure 5: Master Transcription Factor of Tuft Cells *Pou2f3* is upregulated in response to IL-4 in 2D small intestine organoids.** 2D small intestine organoids were made from the small intestines of WT mice. After differentiating for 72 hours, organoids were stimulated with IL-4, poly(dA:dT) encapsulated with lipofectamine (DNA) or lipofectamine-only control (Lipo) for 48 hours. After 48 hours, the cells were then harvested for RNA isolation. \*\*\*\* $p < 0.0001$  and the above graph represents  $n=3$  independent experiments. GraphPad Prism V.9.4.1 was used to generate figure and perform statistical analysis.

## Il13ra1 is upregulated in response to dsDNA Transfection

Once we were able to verify that our 2D organoid system was feasible and demonstrated biological relevance similar to the 3D small intestine organoid system, we then wanted to ask if dsDNA stimulation promoted an increase in associated tuft cell markers. We transfected 2D small intestine organoids with a titration of 0.1-1 ug/ml of the synthetic dsDNA poly(dA:dT) (an activator of AIM2) and measured *Pou2f3* by RT-

qPCR. In contrast to IL-4 stimulation, the dsDNA transfection (regardless of the dsDNA concentration) failed to induce measurable changes in *Pou2f3*. These results have only been investigated within WT organoids up to this point. Further experiments comparing *Aim2*<sup>-/-</sup> organoids would need to be completed in order to confirm that AIM2 promotes tuft cell development in the 2D system.

Because DNA stimulation alone did not induce tuft cells, we hypothesized that AIM2 may promote tuft cells by acting on factors necessary for tuft cell induction, such as upregulating expression of essential receptors. As is noted earlier, IL-13 and IL-4 are type 2 inflammatory cytokines that promote tuft cell differentiation and share receptor components. When both components of the receptor dimerize during cytokine stimulation at the stem cell niche, downstream signaling leads to *Pou2f3* induction and tuft cell differentiation<sup>(11)</sup>. Given this fact, one way that AIM2, and potentially AIM2's dsDNA sensing function, could be promoting tuft cells is through enhanced receptor expression or activation as this is critical to the promotion of tuft cells. It is possible that both components of the receptor *Il4ra* and *Il13ra1* could be pertinent to tuft cell differentiation. Using the 2D small intestine organoid system, we performed dsDNA transfections and measured *Il13ra1* expression by RT-qPCR. 2D small intestine organoids were differentiated for 72 hrs and then transfected with a titration of 0.1-1 ug/ml of poly(dA:dT) encapsulated in lipofectamine for an additional 48 hours. Total RNA was then isolated, and *Il13ra1* expression was measured. In response to dsDNA stimulation, there was a marked increase in *Il13ra1* expression in comparison to the lipofectamine-only control. Lipofectamine alone was to ensure that the lipofectamine itself wasn't responsible for our results. An IL-4 stimulation was also performed as described above. In response to IL-4, *Il13ra1* expression was significantly reduced when comparing to the dsDNA-stimulated organoids. These results lend itself to the idea that dsDNA promotes *Il13ra1* expression, which may enhance the signaling transduction events that allow for tuft cell development.

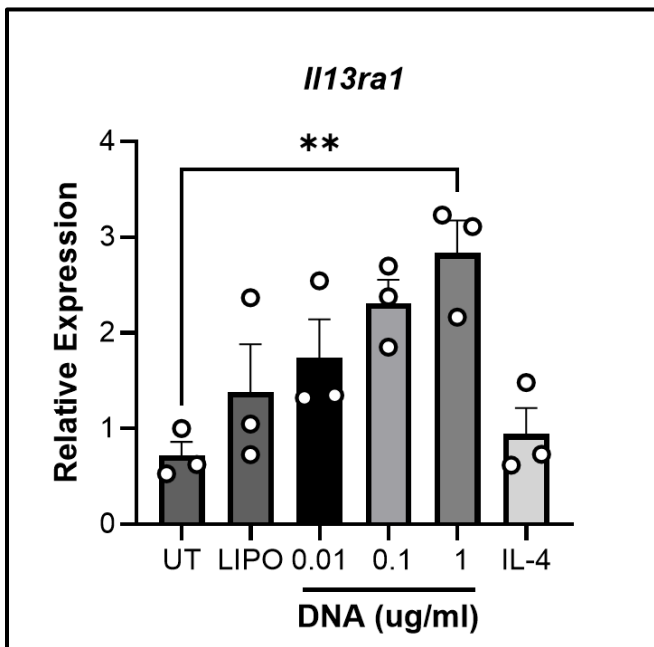


**Figure 6: Associated IL-4 receptor component *IL13ra1* is upregulated in response to dsDNA in 2D small intestine organoids.**

2D small intestine organoids were made from small intestine of WT mice. After differentiating for 72 hours, they were stimulated with IL-4, poly(dA:dT) encapsulated with lipofectamine (DNA) or lipofectamine control (Lipo) for 48 hours. After 48 hours, RNA was isolated from the organoids for qPCR analysis of *IL13ra1*. \*\*p<0.01 and the above graph represents n=3 independent experiments. GraphPad Prism V.9.4.1 was used to generate figure and perform statistical analysis.

## Discussion

Previous research in our lab indicates that *Aim2*<sup>-/-</sup> 3D organoids and succinate-fed mice display a marked decrease in *Dclk1* expression. Given AIM2's primary function is to sense dsDNA, we wanted to investigate if this feature of AIM2 is involved in promoting tuft cells. We established a 2D small intestine epithelial cell organoid system in order to allow for dsDNA transfection. An RNA isolation protocol was also optimized in conjunction with this 2D organoid system. After stimulating the differentiated 2D small intestine organoids with IL-4 for 48 hours, there was a marked increase in *Pou2f3* expression. However, after stimulation with exogenous synthetic dsDNA analog poly(dA:dT) for 48 hours, no significant increase in *Pou2f3* expression was observed. However, stimulating the differentiated 2D small intestine organoids with exogenous poly(dA:dT) for 48 hours, *Il13ra1* expression was markedly increased. These results indicate that dsDNA stimulation may be necessary in order to prime receptors required for the promotion and subsequent differentiation of tuft cells. Thus, DNA stimulation of AIM2 may lead to tuft cell induction in part by promoting the expression of IL-13 receptor.

Key future experiments would involve repeating the dsDNA titration stimulation experiments with both WT and *Aim2*<sup>-/-</sup> 2D small intestine organoids to see if DNA-induced *Il13ra1* expression decreases once AIM2 is lost. If it is true that AIM2 upregulates *Il13ra1* expression, then the next steps after that would be to ask how is AIM2 regulating this receptor expression. One potential avenue to explore this question would be to utilize *Asc*<sup>-/-</sup> 2D small intestine organoids to determine if the AIM2 inflammasome is involved in this process. ASC is a vital protein in the AIM2 inflammasome, thus *Asc*<sup>-/-</sup> 2D small intestine organoids could be used to determine if the formation of the inflammasome is necessary for *Il13ra1* upregulation. However, even if we do not see a difference in *Asc*<sup>-/-</sup> 2D small intestine organoids, AIM2's dsDNA sensing function may still be involved. Currently, there is evidence linking AIM2's inflammasome-independent functions to its dsDNA sensing function, however, this pathway has not been fully characterized<sup>(12)</sup>. Regardless of the outcome, further validation of *Il13ra1* protein levels would be crucial to see if the observed increase in RNA expression leads to increased protein production. To assess this, Western blotting on total protein lysates collected from 2D organoids would be essential. However, further optimization needs to be completed in order to isolate total protein from the 2D organoid cultures. Another important aspect would be to investigate protein localization through microscopy. This would provide validation of how *Il13ra1* receptor is localized after stimulation as well as determining if the actual number of receptors are increased. It would also be pertinent to check for receptor functionality as well. Does a higher number of receptors have an impact on the overall likelihood of increased tuft cell differentiation in response to IL-13? It would be critical to check for protein expression as well for associated tuft cell markers, such as *Dclk1*, after IL-13 stimulation in order to validate functionality in concert with investigating overall receptor numbers.

One area of interest would be to determine if exogenous or endogenous dsDNA promotes AIM2-induced tuft cell differentiation. Although data shown indicates that

exogenous dsDNA transfection doesn't elicit promotion of tuft cells on its own, it does appear to upregulate factors that are necessary for tuft cells. It would be interesting to investigate if a pathogen-associated model versus a damage-associated model would lead to different outcomes for tuft cell numbers. Do external signals for inflammation differ from internal inflammatory signals? Since a key trait of IBD is an abnormal immune response, it would be interesting to see if certain inflammatory signals from various sources, such as bacteria, viruses, or host-derived sources, contribute to that immune response. AIM2 is a pattern recognition receptor that senses dsDNA, which allows it to respond to either a pathogen-derived or host cell sources (particularly during cellular damage). Knowing that AIM2 can sense dsDNA from these distinct sources, would the induction of tuft cells differ when microbial dsDNA is endocytosed into the cell in comparison to nuclear dsDNA leakage from the host cell? AIM2 can sense dsDNA as long as it is approximately 80 base pairs but does not seem to have a particular affinity to where the source of the dsDNA comes from <sup>(13)</sup>. In terms of exogenous dsDNA, there would be two potential avenues to explore. Exogenous dsDNA leakage can come from a microbial source, but also come from neighboring cells who have undergone cell death. To begin look at these differences, it would be ideal to continue with poly(dA:dT) transfection as well as potentially branching out to other forms of synthetic dsDNA as well as infection with intracellular bacteria. Through the exploration of different exogenous dsDNA, we can begin to see if tuft cells are induced in response to either a pathogen-associated model or damage-associated model or if the response is the same between both. Endogenous dsDNA can come from either nuclear dsDNA leakage or mitochondrial dsDNA leakage in response to stress. For endogenous dsDNA, ideally we would use a drug that would either allow for nuclear dsDNA leakage such as Nocodazole, or utilizing Sertraline, a drug that allows mitochondrial dsDNA leakage. Nocodazole is a drug that induces nuclear dsDNA leakage by binding to  $\beta$ -tubulin and disrupting microtubule formation dynamics thus leading to the induction of apoptosis <sup>(14)</sup>. Sertraline is one possible drug that can be utilized in order to induce mitochondrial dsDNA stress thus leading to subsequent dsDNA leakage <sup>(15)</sup>. However, there are other drugs for both nuclear and mitochondrial dsDNA leakage that we would also be willing to explore to see if they would elicit a different response. WT, *Aim2*<sup>-/-</sup>, and *Asc*<sup>-/-</sup> 2D small intestine organoids would be a key choice to address for these questions due to ease of transfection and cellular accessibility, which is hampered by Matrigel in 3D systems. However, *STING*<sup>-/-</sup> 2D small intestine organoids would also be vital in order to ensure that another dsDNA sensing pathway isn't compensating or responsible for the results we are seeing.

One other possible for future research would be to investigate the cell-cell communication between the different intestinal epithelial cell types. It has been previously described for other intestinal epithelial cell types to display this ability. Specifically, sentinel goblet cells can secrete Muc2, which in turn signals to neighboring goblet cells to also secrete Muc2 and ramp up mucus production. This ability of goblet cells is mediated through another inflammasome protein called NLRP6 in response to bacterial components being non-specifically endocytosed into the cell <sup>(16)</sup>. Although the

NLRP6 inflammasome is different than AIM2, the above finding does depict that a relationship may exist between the inflammasome and intestinal epithelial cell communication. The NLRP6 inflammasome is a microbial sensor, while the AIM2 inflammasome is mediated by dsDNA sensing <sup>(17)</sup>. It is possible that dsDNA from a bacterial source instead of host derived source could have a more communicative effect or vice versa. The communicative effect of NLRP6 is based more on a pathogen-associated pattern in comparison to a damage-associated pattern. Therefore, it would be crucial to identify if the cell-cell communication observed is only with pathogen-associated patterns or if a damage-associated model would be able to achieve the same response. Along those same lines, would having a pro-inflammatory response elicit the same features or is this characteristic specific to helping to resolve inflammation and keep a pathogen out? Based off of these findings, it would be interesting to explore whether this communicative feature is specific to goblet cells or if other intestinal epithelial cell types also have this capability. Further investigation of this phenomenon may also prove useful in determining the full picture of the molecular mechanism in how AIM2 may be regulating tuft cell differentiation.

This research is incredibly pivotal because it begins to answer some potential mechanistic questions about how AIM2 may be regulating epithelial cell differentiation. Given that a hallmark trait of IBD is a dysregulation of the intestinal epithelium and abnormal immune function, it is vital to investigate how these cells differentiate and the key players responsible for guiding their respective cell lineages. Based on our results, dsDNA stimulation may be a critical link to the initiation of type 2 immunity and resolution of pathological inflammation in the intestine. By understanding what AIM2's role is in this process during both homeostasis and recovery from inflammation may help lead to treatments for IBD.

## Citations

1. Collaborators, G.B.D.I.B.D., *The global, regional, and national burden of inflammatory bowel disease in 195 countries and territories, 1990-2017: a systematic analysis for the Global Burden of Disease Study 2017*. *Lancet Gastroenterol Hepatol*, 2020. 5(1): p. 17-30
2. Perler, B.K., Ungaro, R., Baird, G. *et al.* Presenting symptoms in inflammatory bowel disease: descriptive analysis of a community-based inception cohort. *BMC Gastroenterol* **19**, 47 (2019). <https://doi.org/10.1186/s12876-019-0963-7>
3. Yamamoto S, Ma X. Role of Nod2 in the development of Crohn's disease. *Microbes Infect.* 2009 Oct;11(12):912-8. doi: 10.1016/j.micinf.2009.06.005. Epub 2009 Jun 30. PMID: 19573617; PMCID: PMC2924159.
4. Hu, S., *et al.*, *The DNA Sensor AIM2 Maintains Intestinal Homeostasis via Regulation of Epithelial Antimicrobial Host Defense*. *Cell Rep*, 2015. 13(9): p. 1922-36.
5. Hornung, V., *et al.*, *AIM2 recognizes cytosolic dsDNA and forms a caspase-1-activating inflammasome with ASC*. *Nature*, 2009. 458(7237): p. 514-8
6. Wilson JE, Petrucelli AS, Chen L, Koblansky AA, Truax AD, Oyama Y, Rogers AB, Brickey WJ, Wang Y, Schneider M, Mühlbauer M, Chou WC, Barker BR, Jobin C, Allbritton NL, Ramsden DA, Davis BK, Ting JP. Inflammasome-independent role of AIM2 in suppressing colon tumorigenesis via DNA-PK and Akt. *Nat Med.* 2015 Aug;21(8):906-13. doi: 10.1038/nm.3908. Epub 2015 Jun 24. PMID: 26107252; PMCID: PMC4529369.
7. Anna Baulies, Nikolaos Angelis, Vivian S. W. Li; Hallmarks of intestinal stem cells. *Development* 1 August 2020; 147 (15): dev182675. doi: <https://doi.org/10.1242/dev.182675>
8. Bonis, Vangelis, *et al.* "The Intestinal Epithelium – Fluid Fate and Rigid Structure from Crypt Bottom to Villus Tip." *Frontiers in Cell and Developmental Biology*, vol. 9, 2021, <https://doi.org/10.3389/fcell.2021.661931>.
9. Lei, W., *et al.*, *Activation of intestinal tuft cell-expressed *Sucnr1* triggers type 2 immunity in the mouse small intestine*. *Proc Natl Acad Sci U S A*, 2018. 115(21): p. 5552-5557.
10. Schneider, C., *et al.*, *A Metabolite-Triggered Tuft Cell-ILC2 Circuit Drives Small Intestinal Remodeling*. *Cell*, 2018. 174(2): p. 271-284 e14
11. Xi, Ranhui, *et al.* "Up-Regulation of Gasdermin C in Mouse Small Intestine Is Associated with Lytic Cell Death in Enterocytes in Worm-Induced Type 2 Immunity." *Proceedings of the National Academy of Sciences*, vol. 118, no. 30, 2021, <https://doi.org/10.1073/pnas.2026307118>.
12. Junjie Zhao, William Miller-Little, Xiaoxia Li; Inflammasome-independent functions of AIM2. *J Exp Med* 3 May 2021; 218 (5): e20210273. doi: <https://doi.org/10.1084/jem.20210273>
13. Jin T, Perry A, Jiang J, Smith P, Curry JA, Unterholzner L, Jiang Z, Horvath G, Rathinam VA, Johnstone RW, Hornung V, Latz E, Bowie AG, Fitzgerald KA, Xiao TS. Structures of the HIN domain:DNA complexes reveal ligand binding and

- activation mechanisms of the AIM2 inflammasome and IFI16 receptor. *Immunity*. 2012 Apr 20;36(4):561-71. doi: 10.1016/j.immuni.2012.02.014. Epub 2012 Apr 5. PMID: 22483801; PMCID: PMC3334467.
14. National Center for Biotechnology Information (2023). PubChem Compound Summary for CID 4122, Nocodazole. Retrieved March 24, 2023 from <https://pubchem.ncbi.nlm.nih.gov/compound/Nocodazole>.
  15. Li Y, Couch L, Higuchi M, Fang JL, Guo L. Mitochondrial dysfunction induced by sertraline, an antidepressant agent. *Toxicol Sci*. 2012 Jun;127(2):582-91. doi: 10.1093/toxsci/kfs100. Epub 2012 Mar 2. PMID: 22387747; PMCID: PMC5736306.
  16. Birchenough, George M., et al. "A Sentinel Goblet Cell Guards the Colonic Crypt by Triggering NLRP6-Dependent muc2 Secretion." *Science*, vol. 352, no. 6293, 2016, pp. 1535–1542., <https://doi.org/10.1126/science.aaf7419>.
  17. Zheng D, Kern L, Elinav E. The NLRP6 inflammasome. *Immunology*. 2021 Mar;162(3):281-289. doi: 10.1111/imm.13293. Epub 2020 Dec 27. PMID: 33314083; PMCID: PMC7884648.